Biosensors and Bioelectronics 24 (2008) 104–110

Contents lists available at ScienceDirect

Biosensors and Bioelectronics

journal homepage: www.elsevier.com/locate/bios

Impedance studies of a nano-structured conducting polymer and its application to the design of reliable scaffolds for impedimetric biosensors

Mojtaba Shamsipur[a,*], Sayed Habib Kazemi[b], Mir Fazlollah Mousavi[b]

[a] Department of Chemistry, Razi University, Kermanshah, Iran
[b] Department of Chemistry, Tarbiat Modares University, Tehran, Iran

ARTICLE INFO

Article history:
Received 15 January 2008
Received in revised form 3 March 2008
Accepted 19 March 2008
Available online 1 April 2008

Keywords:
Nano-structure
Conducting polymer
Impedance
Cytochrome *C*
Biosensor
Hydrogen peroxide

ABSTRACT

Electrochemical impedance spectroscopy (EIS) as a powerful, non-invasive and informative technique was used to obtain important information about kinetics of doping process in conducting polymers. Polypyrrole (PPy) and its derivatives can form conducting polymer films which represent excellent charge transfer behaviors during doping processes. It can also have a wide range of applications in bioelectrochemistry. In the present study the conducting polymer of α-carboxy pyrrole (α-COOH-PPy), appended onto the underlying film of PPy, was prepared by electrochemical methods and its behavior was analyzed using EIS. From highly accurate fitting of impedance results it was found that the charging mechanism is governed by the diffusion process. In addition, the impedance analyses provided values for the bulk polymer parameters including diffusion coefficient (D), equilibrium capacitance (C_0) and diffusion resistance (R_0). The surface morphology of the polymeric film was characterized using scanning electron microscopy (SEM). The film was then used to immobilize the cytochrome *C* (cyt-*C*) and to perform its electrochemical studies. The modified cyt-*C*/α-COOH-PPy electrode was used for electrocatalytic reduction of H_2O_2 in solution and its viability as a new impedimetric biosensor was examined. Based on the calibration curve obtained for the proposed impedimetric biosensor, the limit of detection and relative standard deviation were evaluated as 0.25 μmol L^{-1} and 7%, respectively. Finally, the prolonged stability test was performed and high stability and reproducibility of the new biosensor was confirmed.

1. Introduction

Studies of electroactive materials and especially thin films deposited onto the electron conducting surfaces are of increasing interest in electrochemistry due to construction of a broad range of materials for applications in photovoltaics, catalysis, energy storage systems (supercapacitors and rechargeable batteries), chemical and biological sensors and biophysics (Popkirov et al., 1997; Belmonte and Bisquert, 2002; Belmonte, 2003). Finding the fact that certain classes of polymers may acquire high electronic conductivity, both chemically and electrochemically treated, has opened an exciting area of research and development. The concept of electrical transport in polymers due to the availability of polymeric materials is certainly fascinating. Indeed, many studies have been directed towards the preparation and characterization of these new electroactive conductors to be used as new components for the realization of electronic and electrochemical devices with exotic designs and diverse applications (Bruce, 1995).

Among different conducting polymers, polypyrrole (PPy) is well-known as a conductive biocompatible polymer with the potential to bring the benefits of conductivity into tissue-engineered constructs (Adeloju and Wallace, 1996; Ateh et al., 2007; Bardavid et al., 2006; Peng et al., 2007; Gu et al., 2005). In addition, PPy presented some important characteristics like dopant-mediated tunable physical properties and good stability in air and aqueous media. In the future, it is expected that the conducting polymers based biomedical devices will likely find specific therapeutic applications in *in vivo* drug delivery and use as bioanalytical microelectrodes. An important point to be considered in a drug delivery system is its biocompatibility. Since the conducting polymers based on pyrrole derivatives possess low cytotoxicity and are stable to a broad selection of redox and acid–base conditions, many efforts have been carried out to design reliable and remarkable biological scaffolds and sensors using PPys (Sanchis et al., 2007; Malhotra et al., 2006; Biallozor and Kupniewska, 2005; Ahujaa et al., 2007).

* Corresponding author. Tel.: +98 21 66908032; fax: +98 21 66908030.
E-mail address: mshamsipur@yahoo.com (M. Shamsipur).

0956-5663/$ – see front matter © 2008 Elsevier B.V. All rights reserved.
doi:10.1016/j.bios.2008.03.028

Different procedures have been used to immobilize the biomolecules, especially macromolecules, onto the conductive polymer substrates (Ahujaa et al., 2007; Hudson et al., 2005). The main immobilization methods include covalent immobilization, affinity interactions and entrapment of biological species. It should be stressed that covalent immobilization and entrapment of proteins and enzymes may not only change their activity but also will result in structural denaturation. On the other hand, although the immobilization through physical adsorption suffers from some drawbacks like poor stability and inappropriate long life, its main advantage is less denaturing effects on the protein structure.

Cytochrome *C* (cyt-*C*) is one of the most important mitochondrial proteins playing vital roles in the living cells (Ateh et al., 2007; Bardavid et al., 2006). It is a relatively simple metalloprotein comprising only 104 amino acids, which is used as a prototypical metalloprotein. The electrochemical studies on cyt-*C* have been carried out onto several different substrates (Murgida and Hildebrandt, 2004; O'Reilly and Magner, 2005; Jiang et al., 2005). However, the adsorption process is shown to result in large changes in cyt-*C* conformation and often results in denaturation of the protein. To triumph over these failings, several efforts have been done including the use of SAMs and thin conductive film for cyt-*C* immobilization especially based on electrostatic interactions (Darain et al., 2007; Deshpande and Amalnerkar, 1993; Trojanowicz, 2003; Zhang et al., 2006; Sugihara et al., 1998).

In the present work, a carboxy endcapped polymeric structure was prepared through electropolymerization of α-carboxypyrrole onto a thin film of polypyrrole, prepared using the C–C coupling (Lee et al., 2006), and its electrochemical behavior was studied using electrochemical impedance spectroscopy (EIS) method. In contrast to cyclic voltammetry, impedance spectroscopy uses a small-amplitude perturbation signal; thus, it is an excellent tool for obtaining highly resolved kinetic data related to thin films of electroactive polymers (Levi and Aurbach, 2002; Macdonald, 2006). In addition, cyt-*C* was immobilized onto the prepared thin film and its electrochemical behavior towards H_2O_2 was investigated. The results clearly revealed that the immobilized cyt-*C* onto the carboxy endcapped polymer can be used as an impedimetric biosensor for the determination of the H_2O_2 concentration.

2. Materials and methods

2.1. Reagents and apparatus

All reagents were of analytical grade from Aldrich Chemical Company. Bovine heart cyt-*C* was purchased from Sigma and used without any further purification. Reagent grade organic solvents were obtained from Merck Company. All solutions were degassed after preparation, and prior to each experiment. The protein solutions stored at 4 °C. The working electrode was a 2 mm diameter Pt disc, and a 2 cm^2 area Pt counter electrode and an Ag/AgCl, KCl (saturated) reference electrode were used, with the double junction filled with a proper supporting electrolyte solution in each case. These experiments were carried out on an Autolab30 Potentistat-Galvanostat system (Eco Chemie, B. V. Utrecht, The Netherlands), supplied with FRA2 module boards. The system was run by a personal computer (PC) through FRA and GPES 4.9 software. The SEM micrographs were prepared with a Philips instrument.

2.2. Electrochemical polymerization and characterizations

Before electropolymerization, the electrode surface was polished with 1 and 0.05 μm alumina powders until a mirror-like surface was obtained. Then, it was sonicated in ethanolic solution at least for 10 min. The electropolymerization was carried out in two steps according to a previously reported method (Lee et al., 2006). The electropolymerization was followed in a conventional three electrode cell in 0.1 mol L^{-1} pyrrole in acetonitrile, containing 0.1 mol L^{-1} of $LiClO_4$ as supporting electrolyte, to prepare a thin film of polypyrrole. Pulse chronoamperometry with an offset potential of 800 mV was used to afford this step. Then, the prepared electrode was introduced to a cell solution of 0.1 mol L^{-1} of α-carboxypyrrole in acetonitrile containing 0.1 mol L^{-1} of $LiClO_4$, and an offset potential of 2 V was applied for at least 10 min to ensure the α-terminus C–C coupling between PPy and α-COOH-Py (Lee et al., 2006). A cartoon representation of the conducting film is demonstrated in Scheme 1. All the measurements were done at ambient temperature. The uniformity and nano-structural properties of the surface were examined using SEM analysis.

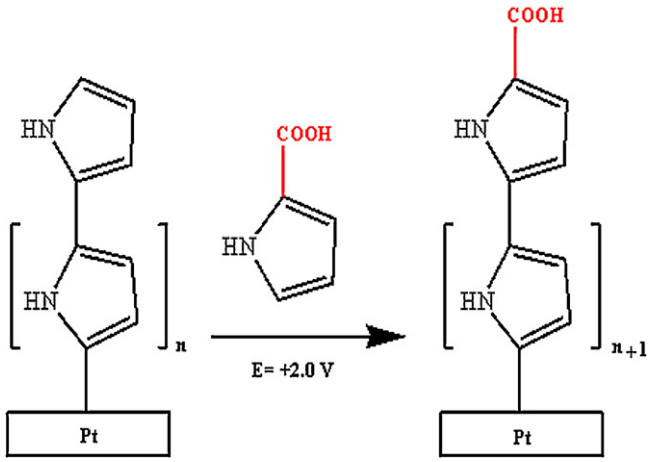

Scheme 1. Cartoon representation of the carboxy endcapped PPy formed from electropolymerization of α-COOH-Py onto the PPy film.

2.3. Immobilization of cyt-C onto the polymeric film

A 1000 μg mL^{-1} stock solution of cyt-*C*, in a 0.1 mol L^{-1} phosphate buffer solution of pH 5, was prepared and stored at 4 °C to avoid its denaturation. Incubation of the polymer-coated surface with this solution was performed overnight. After that, the electrodes were washed thoroughly with doubly distilled water to remove physically adsorbed macromolecules and finally introduced to the cell.

2.4. Impedance measurements

Impedance measurements were carried out in a conventional three-electrode electrochemical cell in two parts. First, the electrochemical studies of polymeric film were done in an acetonitrile solution containing $LiClO_4$ as supporting electrolyte, from 100 kHz to 0.01 Hz. Then, the EIS studies of the modified cyt-*C*/α-COOH-PPy electrode was carried out in a 0.1 mol L^{-1} of phosphate buffer solution of pH 5 to investigate the electrocatalytic behavior of immobilized cyt-*C* at the polymer surface towards H_2O_2. A modulation signal of 10 mV amplitude was used to perturb the electrical behavior in these experiments and at least seven points per decade, equally spaced on a logarithmic scale, were obtained. The impedance data were fitted with a proper electrical equivalent circuit using the complex nonlinear least square (CNLS) method for impedance fitting.

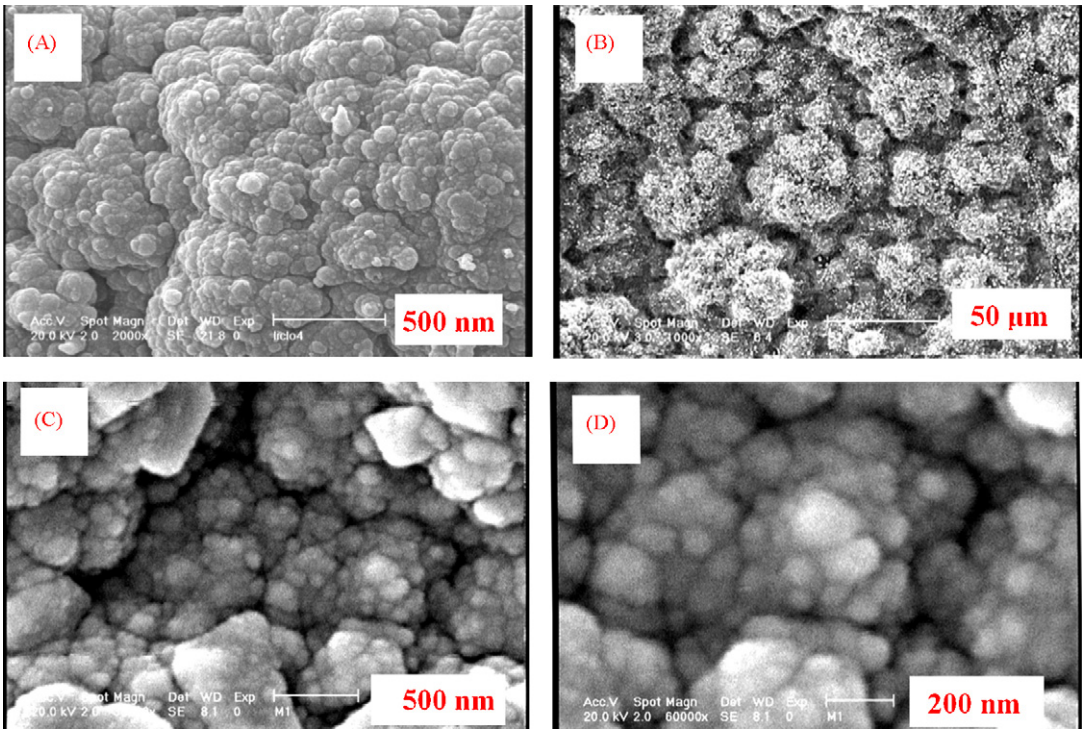

Fig. 1. SEM images of the electrode surface modified with PPy (A) and different magnifications of the α-COOH-PPy modified electrode surface (B–D).

3. Results and discussion

3.1. Polymer synthesis and surface characterization

Fig. 1 shows the SEM images of the PPy and α-COOH-PPy prepared in the present work. Obviously, the SEM results revealed that both PPy and α-COOH-PPy modified electrodes represent homogenous nano-structures, as reported previously (West et al., 2004; Lee and Park, 2005). As seen, morphology of the PPy polymer film is of cauliflower shape and the final α-COOH-PPy film is also of cauliflower shape but with more globular morphology. It is worth mentioning that the overall structure of the thin film is mostly dependant on the PPy underlayer and, thus, there should be only slight changes in the final carboxy end-capped surface at high positive voltages. Additionally, the film thickness is determined by the number of multiple pulses used in the process of preparation of the PPy under-layer. Based on the charge passed through the synthesis of PPy ($\leq$60 mC cm^{-2}), the film thickness was estimated as 200 nm. Of course, the under-layer PPy is a uniform electrodeposited layer as normally prepared for other applications, but the modification of the final surface with the carboxy endcapped monolayer is its novelty to use as a bio-scaffold.

The electrochemical cycling of the conducting polymer film in a 0.1 M $LiClO_4$ solution revealed stable and reproducible peaks and the bias dc potentials used for impedance analyses were chosen based on the doping–undoping voltammograms.

3.2. Impedance analysis of α-COOH-PPy polymer film

It is reported that several mechanisms determine the doping kinetics in the conducting polymers, namely, interfacial electronic and charge transfer, double layer capacitance, charging capacity, ionic and electronic diffusion in the polymer film and electrode morphology (Belmonte et al., 2004). It is well known that, for the case of ordinary diffusion-controlled systems, semi-infinite diffusion would appear in the frequency domain determined by the following equation (Bisquert, 2002; Pitarch et al., 2004):

$$Z = K(\mathrm{i}\omega)^{-0.5} \quad (1)$$

However, some other processes may influence the ordinary diffusion behavior, especially in the case of conducting polymers and semiconductor materials. Recently, new approaches have been developed in the case of such deviated and anomalous diffusion behavior (Bisquert et al., 1998; Bisquert et al., 1999; Belmonte et al., 2004; de Levie, 1963), in which the following fractional diffusion equation has been suggested:

$$\frac{\partial^{\gamma} C}{\partial t^{\gamma}} = -\frac{\partial J}{\partial x} \quad (0 < \gamma \leq 1) \quad (2)$$

In which, $\gamma = 1$ represents the case of normal conservation law and results in ordinary diffusion. Using the Fick's laws together with the Laplace transformation method for this case resulted in the following diffusion element:

$$Z_{\mathrm{D}} = R_{\mathrm{d}} \left(\frac{\mathrm{i}\omega}{\omega_{\mathrm{d}}} \right)^{-\gamma/2} \coth \left[\left(\frac{\mathrm{i}\omega}{\omega_{\mathrm{d}}} \right)^{\gamma/2} \right] \quad (3)$$

In this equation ω_{d} is a characteristic frequency where transition between Warburge and capacitive-like behavior will observed, ω is the angular frequency and R_{d} is a diffusion resistance.

At high frequency region, Eq. (3) gives a straight line inclined at less than 45°; this equation is also similar to the thin layer behavior with reflecting boundary, and different boundary conditions, in comparison to semi-infinite diffusion. The diffusion element Z_{D}, which described the ionic diffusion and charging the film, has already been used to fit the diffusion process in some of the conducting polymer films (Belmonte et al., 2004). It was reported that, at lower frequencies (i.e., <1000 Hz), the spectra is dominated by the spatially restricted diffusion element (Z_{D}), and the doping kinetics always limited to the lower frequencies mentioned above. In addition, different models have been used to evaluate the kinetics of

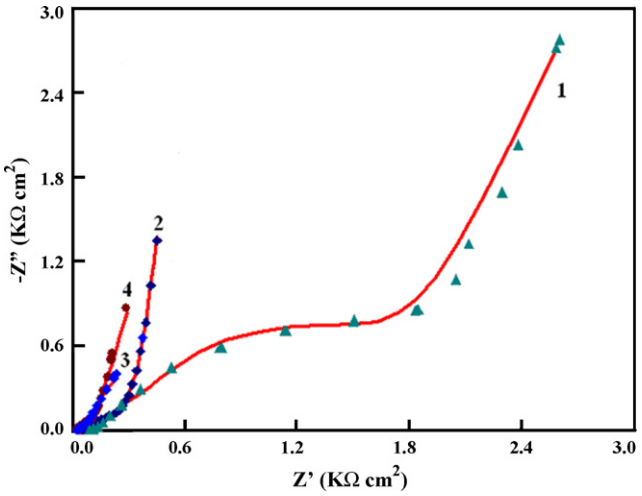

Fig. 2. Nyquist plots obtained for α-COOH-PPy electrode at different offset potentials in solutions containing 0.1 mol L^{-1} of $LiClO_4$. The offset potentials used are: −0.25 V (1), 0.0 V (2), 0.1 V (3), +0.25 V (4). Points are the experimental data and the lines show the fitted results.

doping process in PPy conducting polymers by Levi and Aurbach, including the finite space Warburge (Levi and Aurbach, 2002).

Fig. 2 shows the Nyquist plots obtained for the α-COOH-PPy film in 0.1 mol L^{-1} solution of $LiClO_4$ at different offset potentials. Herein, we used the CNLS fitting method to analyze the impedance behavior of the proposed conductive film. From the viewpoint of electrical circuit, the best analogy to this problem can be considered as transmission lines for ordinary diffusion process in which *C* is replaced with constant phase element (CPE).

All of the experimental results shown in Fig. 2 were fitted using the mentioned diffusion element in series with resistance of solution. The electrical parameters calculated are given in Table 1. Furthermore, it is possible to find the characteristic diffusion frequency, ω_d, as a useful parameter to determine the chemical diffusion coefficient, as:

$$\omega_d = \frac{D^2}{L} \tag{4}$$

It should be noted that, in the present study, *D* is considered as effective diffusion coefficient, $D = D_e D_i/(D_e + D_i)$, in which D_e and D_i are the partial diffusion coefficient for polarons and ions, respectively, as the main carriers in polymeric matrix, and *L* is the diffusion length or diffusion thickness; thus, the slow carriers (i.e., the ionic species) play a major role in the effective diffusion coefficient (Levi and Aurbach, 2002; Belmonte et al., 2004). The chemical diffusions evaluated for the α-COOH-PPy film in the present work, for different film thicknesses, were almost the same.

The kinetic parameters equilibrium bulk capacitance, C_0, and diffusion specific resistance, R_0, evaluated from the impedance analysis of the α-COOH-PPy films are also included in Table 1. The equilibrium bulk capacitance may be estimated from the capacitive characteristics of low frequency region of the Nyquist plots as:

$$C_0 = \frac{C_{Lf}}{AL} \tag{5}$$

where *A* is the active surface area of the film and C_{Lf} is the low frequency capacitance (Belmonte et al., 2004). Also, R_0 could be estimated as follows:

$$R_0 = \frac{R_d A}{L} \tag{6}$$

where R_d is a diffusion resistance (see Eq. (3)).

3.3. Voltammetric behavior of cyt-C immobilized α-COOH-PPy

Fig. 3A shows the cyclic voltammograms recorded for the case of α-COOH-PPy (1) and cyt-*C*/α-COOH-PPy (2) modified electrodes in a 0.1 mol L^{-1} phosphate buffer solution of pH 5. No obvious response can be found before modification of the surface with cyt-*C* (voltammogram 1), but a couple of stable redox peaks appeared in the region of 0 to −0.1 V for the cyt-*C*/α-COOH-PPy electrode (voltammogram 2). Clearly, these peaks are attributed to the redox reaction of the electroactive center of cyt-*C*.

It seems that the adsorption of cyt-*C* on the α-COOH-PPy surface resulted in improving electron transfer between the electroactive center of protein and the underlying electrode surface. The $E_{1/2}$ for cyt-*C* can be approximately estimated as −30 mV. Small deviations in redox peak potentials, in comparison to the bare electrode, can be attributed to the interaction of protein molecules and underlying polymeric film (Darain et al., 2007). In addition, the electrochemical behavior of the attached layer shows a quasi-reversible behavior so that the anodic to cathodic current ratio approximately equals to unity. Meanwhile, the peak-to-peak separation is larger than that expected for the case of a totally reversible behavior for the surface confined systems, which can be attributed to the presence of some kinetic limitations.

In order to investigate the characteristics of the attached layer, the effect of potential scan rate on the peak current was examined and the results are demonstrated in the inset of Fig. 3B. The dependency of peak current as a function of scan rate is shown as an inset in Fig. 3B. As seen, the redox peak currents of the immobilized cyt-*C* on the polymeric film are increased linearly with scan rate indicating a surface-controlled electrode process. An average surface coverage of cyt-*C* on the polymeric film of 1.34×10^{-10} mol cm^{-2} was evaluated from the reduction peak of cyt-*C* shown in the inset, at different scan rates.

3.4. Electrocatalysis of cyt-C/α-COOH-PPy towards reduction of H_2O_2

3.4.1. Voltammetric studies

As it is seen from Fig. 3C, upon addition of H_2O_2 to a 0.1 mol L^{-1} of phosphate buffer solution of pH 5, the shape of cyclic voltammogram for the direct electron transfer to the immobilized cyt-*C* (cyt-*C*/α-COOH-PPy), the cathodic current was dramatically increased in the expense of the decreased oxidation current. As is

Table 1
Electrochemical and diffusion parameters obtained from fitting of the experimental results of polymer film at different potentials (x_1 and x_2 stand for constant phase elements used in the equivalent circuit to perform CNLS)[a]

	R_d (Ω)	$10^3 C_{\times 1}$ (F)	$n_{\times 1}$	$10^3 C_{\times 2}$ (F)	$n_{\times 2}$	$10^{-9} D$ (cm s^{-1})	$10^6 R_0$ (Ω cm))	C_0 (F cm^{-3})
OCP	304 ± 12	4.0 ± 0.2	0.93 ± 0.04	3.8 ± 0.2	0.87 ± 0.04	1.0 ± 0.1	110.6 ± 6.1	53 ± 3
−0.25 V	1319 ± 53	1.3 ± 0.1	0.78 ± 0.03	1.9 ± 0.1	0.96 ± 0.04	3.2 ± 0.2	20.1 ± 1.3	105 ± 6
0.1 V	144 ± 6	4.0 ± 0.2	0.73 ± 0.03	7.4 ± 0.3	1.00 ± 0.04	5.0 ± 0.3	1.6 ± 0.1	211 ± 11
0.25 V	111 ± 4	3.4 ± 0.1	0.47 ± 0.02	11.1 ± 0.4	0.98 ± 0.04	8.5 ± 0.6	0.20 ± 0.02	398 ± 20

[a] All data points are associated with ± S.D. for five replicate determinations.

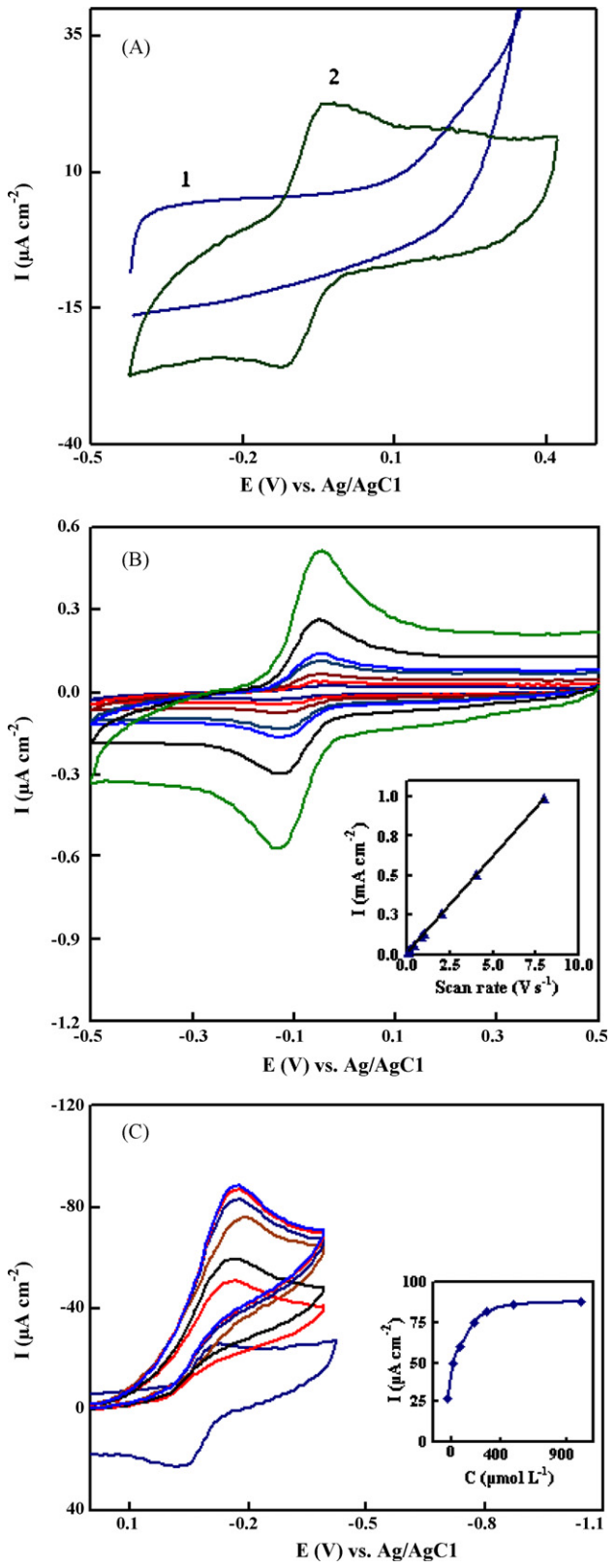

Fig. 3. (A) Cyclic voltammograms recorded for the case of α-COOH-PPy (1) and cyt-*C*/α-COOH-PPy (2) modified electrodes in a 0.1 mol L^{-1} phosphate buffer solution of pH 5. (B) Successive cyclic voltammograms obtained at different scan rates, from 0.1 to 8 V s^{-1}, for the cyt-*C*/α-COOH-PPy electrode. Inset shows the corresponding linear plot of current vs. scan rate. (C) Cyclic voltammograms recorded for the case of cyt-*C*/α-COOH-PPy electrode in a 0.1 mol L^{-1} phosphate buffer solution of pH 5 after addition 0, 50, 100, 200, 400, 800 and 1000 μmol L^{-1} of H_2O_2 (from bottom to top).

obvious from Fig. 3C, upon an increase in concentration of H_2O_2, the anodic peak, is gradually disappeared in the expense of a dramatic increase in the cathodic peak; the observed voltammetric behavior being characteristic of a catalytic mechanism (EC′) for the reaction. The variation of peak currents with the H_2O_2 concentration is shown as an inset in Fig. 3C. As seen, the successive addition of H_2O_2 concentration up to the 1 mmol L^{-1} resulted in a continuous increase in the reductive peak (Fig. 3C).

As expected, in other experiments, it was found that the changes in voltammogram of the α-COOH-PPy electrode (in the absence of cyt-*C*) is insignificant, supporting a typical electrocatalytic behavior for cyt-*C* towards H_2O_2 reduction. Furthermore, an increase in the potential scan rate, in the presence of a constant concentration of H_2O_2, resulted in an increased reductive peak current proportional to the square root of scan rate. This is an indication for the fact that the reduction of H_2O_2 onto the cyt-*C*/α-COOH-PPy is relatively fast and the process is controlled by the rate of diffusion of H_2O_2 to the electrode surface (results are not shown here).

3.4.2. Impedance studies

In order to design an impedimetric biosensor, it is necessary to find an appropriate relationship between electrical response of the modified surface in the absence and presence of the species of interest (Cortina-Puig et al., 2007; Ateh et al., 2007). Thus, the offset potential was set at −0.4 V vs. Ag/AgCl electrode to ensure the regeneration of the reductive form of the immobilized cyt-*C*. Additionally, the application of a negative potential will lead to a better interaction between cyt-*C* and negatively charged polymer surface, as well as a partial dissociation of the carboxylic group at the outer surface of the polymer. It has been reported that H_2O_2 molecules diffuse towards the modified surfaces and, subsequently, electron transfer will occur from the protein centers to the H_2O_2 molecules (Liu et al., 2007).

The EIS results obtained in the absence and presence of increasing concentration of hydrogen peroxide at the surface of the modified cyt-*C*/α-COOH-PPy electrode are shown in Fig. 4A. The Nyquist plot obtained in the absence of H_2O_2 (Fig. 4A, plot 1) illustrates the electrochemical behavior of cyt-*C* at the polymer surface with an offset potential of −0.4 V. As seen, after immobilization of the protein on polymer surface, the impedance behavior of surface is changed to an extensive semicircle in the Nyquist plots. This semicircle can be attributed to the cyt-*C*-Fe^{3+} reduction to the cyt-*C*-Fe^{2+}. This fact was supported by performing a controlled experiment, in which instead of its immobilization onto the surface, cyt-*C* was dissolved in the electrolyte solution and the corresponding Nyquist plot was obtained. The resulting plot revealed a pattern similar to that of the modified cyt-*C*/α-COOH-PPy electrode (Fig. 4A), supporting the fact that the resulting semicircle is due to the cyt-*C*-Fe^{3+} reduction to cyt-*C*-Fe^{2+}at the α-COOH-PPy electrode.

Furthermore, the modified electrode was introduced into solutions containing varying concentrations of H_2O_2 and the results are also shown in Fig. 4A, plots 2–8. As it is obvious, the semicircle began to change and its diameter was gradually decreased with increasing concentration of H_2O_2. In addition, in all of the Nyquist plots obtained for different concentrations of H_2O_2, the observation of an almost straight portion at the low frequency region indicates the occurrence of a diffusion-controlled process. More detailed EIS experiments in the present study revealed that extending the frequency region to the lower limits results in straight lines with slope of unity, related to diffusion-controlled element or Warburg impedance. This finding is clearly confirmed the results obtained by voltammetric method (Section 3.4.1.). The electrical parameters were evaluated based on the fitting of experimental results to an appropriate Randles equivalent circuit shown

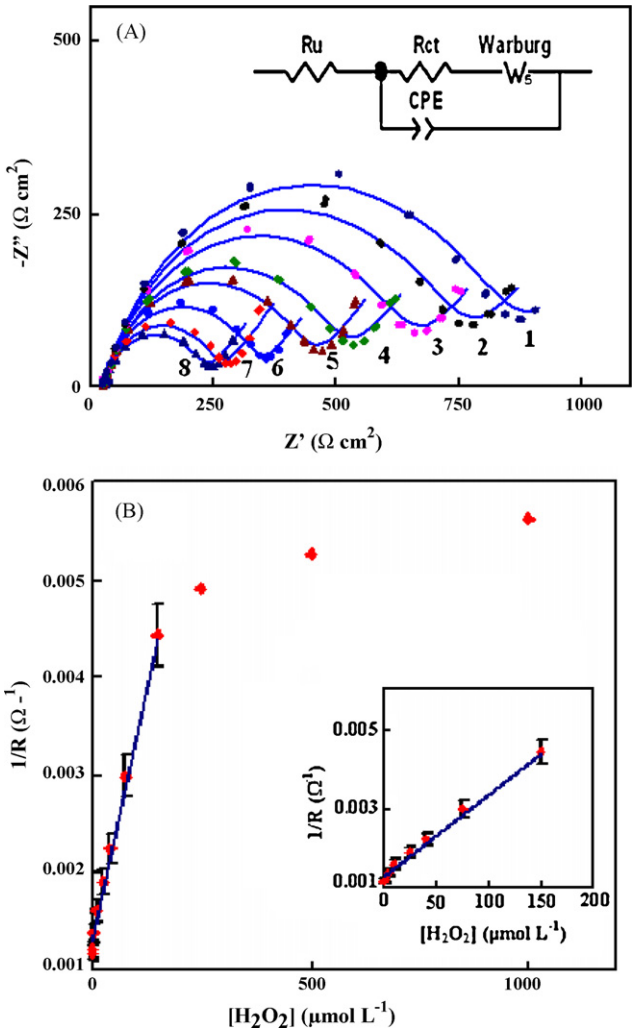

Fig. 4. (A) Nyquist plots obtained for cyt-*C*/α-COOH-PPy electrode in a 0.1 mol L^{-1} phosphate buffer solution of pH 5 in the presence of 0, 1, 5, 20, 50, 100, 150, 200 μmol L^{-1} of H_2O_2 (denoted as 1–8). The inset shows equivalent circuit used to fit the experimental results of the electrochemical reduction of H_2O_2 at cyt-*C*/α-COOH-PPy electrode. (B) The reciprocal of charge transfer resistance vs. [H_2O_2] calibration curve obtained for the cyt-*C*/α-COOH-PPy electrode in a 0.1 mol L^{-1} phosphate buffer solution of pH 5. Inset shows the linear dynamic range used to evaluate LOD for biosensor.

in the inset of Fig. 4A. In order to evaluate the analytical concepts from this relationship, the charge transfer resistances were calculated by fitting the impedance data to the proposed equivalent circuit (see inset of Fig. 4A), using the CNLS fitting method. Then, the reciprocal of charge transfer resistances were plotted against the H_2O_2 concentration and the resulting plot is shown in Fig. 4B.

As it is seen, the linear dynamic range of the proposed impedimetric sensor is 1–200 μmol L^{-1} with a calibration sensitivity of 2.0×10^{-5} Ω^{-1} μmol L^{-1}. The limit of detection, LOD, and relative standard deviation, R.S.D., for five replicate determinations for the proposed biosensor were calculated as 0.25 μmol L^{-1} and 7%, respectively. In addition, the stability test was performed to estimate the stability and durability of the newly constructed biosensor under the storage conditions. After 10 days, the biosensor preserves almost 95% of its initial response, which revealed that the cyt-*C*/α-COOH-PPy biosensor has adequate stability with time. These characteristics are comparable with and in some cases are superior to those of the H_2O_2 biosensors previously reported in the literature (Liu et al., 2007; Lei and Deng, 1996; Yu and Ju, 2002; Dai et al., 2004; Liu et al., 2004).

4. Conclusions

A conductive polymer film of α-COOH-PPy was prepared onto a PPy film using the electrochemical methods. Impedance analysis of this film was performed based on the concept of fractional diffusion equations for anomalous diffusion processes. Some of the kinetic parameters were evaluated by means of EIS. Subsequently, the film was used as a scaffold to immobilize cyt-*C* and to develop a novel biosensor. The facilitated electron transfer of cyt-*C* in addition to its intrinsic catalytic behavior afforded a new route for H_2O_2 determination. Studies on the direct electron transfer of the immobilized cyt-*C* onto the α-COOH-PPy film opened an effective way to construct a novel H_2O_2 biosensor with good sensitivity, dynamic range, detection limit (LOD) and long life. More importantly, the present study provided a methodology to design impedimetric biosensors based on the polymeric films which can be easily formed on the electrode surfaces. Another advantage of the present work is to overcome the previously reported drawbacks like poor stability and inappropriate long life in addition of less denaturing effects on the protein structure. More investigations on the design of cyt-*C* modified α-COOH-PPy films using other immobilization procedures are underway in our research group.

Acknowledgement

The support of this work by a research grant (no. 84123/17) from Iran National Science Foundation (INSF) is gratefully acknowledged.

References

Adeloju, S.B., Wallace, G.G., 1996. Analyst 121, 699–703.
Ahujaa, T., Mira, I.A., Rajesh, D.K., 2007. Biomaterials 28, 791–805.
Ateh, D.D., Waterworth, A., Walker, D., Brown, B.H., Navsaria, H., Vadgama, P., 2007. Journal of Biomedical Materials Research Part A 83A, 391–400.
Bardavid, Y., Kotlyar, A.B., Yitzchaik, S., 2006. Macromolecular Symposium 240, 102–106.
Belmonte, G.G., Bisquert, J., 2002. Electrochimica Acta 47, 4263–4272.
Belmonte, G.G., 2003. Electrochemistry Communication 5, 236–240.
Belmonte, G.G., Pomerantz, Z., Bisquert, J., Lellouche, J.P., Zaban, A., 2004. Electrochimica Acta 49, 3413–3417.
Biallozor, S., Kupniewska, A., 2005. Synthetic Metals 155, 443–449.
Bisquert, J., Belmonte, G.G., Santiago, F.F., Compte, A., 1999. Electrochemistry Communication 1, 429–435.
Bisquert, J., Belmonte, G.G., Bueno, P., Longo, E., Bulhoes, L.O.S., 1998. Journal of Electroanalytical Chemistry 452, 229–234.
Bisquert, J., 2002. Journal of Physical Chemistry B 106, 325–333.
Bruce, P.G., 1995. Solid State Electrochemistry. Cambridge University Press.
Cortina-Puig, M., Berbel, X.M.M, Lomillo, A.A., Pascual, F.J.M., Valle, M.D., 2007. Talanta 72, 774–779.
Dai, Z., Liu, S., Ju, H., 2004. Electrochimica Acta 49, 2139–2144.
Darain, F., Park, J.S., Akutsu, H., Shim, Y.B., 2007. Biosensors and Bioelectronics 23, 161–167.
de Levie, R., 1963. Electrochimica Acta 8, 751–780.
Deshpande, M.V., Amalnerkar, D.P., 1993. Progress in Polymer Science 18, 623–649.
Gu, H., Su, X., Loh, K.P., 2005. Journal of Physical Chemistry B 109, 13611–13618.
Hudson, S., Magner, E., Cooney, J., Hodnett, B.K., 2005. Journal of Physical Chemistry B 109, 19496–19506.
Jiang, X., Shang, L., Wang, Y., Dong, S., 2005. Biomacromolecules 6, 3030–3036.
Lee, H.J., Park, S.M., 2005. Journal of Physical Chemistry B 109, 13247–13254.
Lee, J.W., Serna, F., Schmidt, C.E., 2006. Langmuir 22, 9816–9819.
Lei, C., Deng, J., 1996. Analytical Chemistry 68, 3344–3349.
Levi, M.D., Aurbach, D., 2002. Journal of the Electrochemical Society 149, E215–E221.
Liu, S., Dai, Z., Chen, H., Ju, H., 2004. Biosensors and Bioelectronics 19, 963–969.
Liu, H., Tian, Y., Deng, Z., 2007. Langmuir 23, 9487–9494.
Macdonald, D.D., 2006. Electrochimica Acta 51, 1376–1388.
Malhotra, B.D., Chaubey, A., Singh, S.P., 2006. Analytica Chimica Acta 578, 59–74.
Murgida, D.H., Hildebrandt, P., 2004. Accounts of Chemical Research 37, 854–861.

O'Reilly, N.J., Magner, E., 2005. Langmuir 21, 1009–1014.
Peng, H., Soeller, C., Sejdic, J.T., 2007. Macromolecules 40, 909–914.
Pitarch, A., Belmonte, G.G., Sero, I.M., Bisquert, J., 2004. Physical Chemistry Chemical Physics 6, 2983–2988.
Popkirov, G.S., Barsoukov, E., Schindler, R.N., 1997. Journal of Electroanalytical Chemistry 425, 209–216.
Sanchis, C., Salavagione, H.J., Arias-Pardilla, J., Morallon, E., 2007. Electrochimica Acta 52, 2978–2986.
Sugihara, N., Ogoma, Y., Abe, K., Kondo, Y., Akaike, T., 1998. Polymers for Advanced Technologies 9, 307–313.
Trojanowicz, M., 2003. Microchimica Acta 43, 75–91.
West, K., Bay, L., Nielsen, M.M., Velmurugu, Y., Skaarup, S., 2004. Journal of Physical Chemistry B 108, 15001–15008.
Yu, J., Ju, H., 2002. Analytical Chemistry 74, 3579–3583.
Zhang, L., Jiang, X., Niu, L., Dong, S., 2006. Biosensors and Bioelectronics 21, 1107–1115.